ELECTRONIC SUPPORTING INFORMATION

for

Linear and Circular Dichroism in Porphyrin J-Aggregates Probed by Polarization Modulated Scanning Near-Field Optical Microscopy

Francesco Tantussi, Francesco Fuso, Maria Allegrini, Norberto Micali, Ilaria Giuseppina Occhiuto, Luigi Monsù Scolaro, Salvatore Patanè**

The apparatus for the nanoscale analysis of the optical activities is based on a Scanning Near-Field Optical Microscope (SNOM) operating in emission mode.[S1] Tapered, metal coated, optical fiber probes (LovaLite E50-MONO) are used as a quasi-point-like near-field source, which is made to interact with the sample surface, being the tip-to-surface distance kept in the few nanometers range by the shear-force method.[S2]

The optical signal is collected in the far-field by an aspheric lens placed below the sample and sent onto a miniaturized photomultiplier tube (Hamamatsu R-7400) housed inside the hollow-tube piezoelectric scanner used for moving the sample with respect to the probe. The output of the photomultiplier tube is split and sent to the current input of two distinct dual lock-in amplifiers (Stanford Research SR830DSP). Depending on the specific measurement to be carried out, the lock-ins are referenced to different signals. For instance, for the optical maps representing the optical activity at the nanoscale, the reference is synchronous to the polarization modulation, occurring at frequency f = 50 kHz. When polarization-averaged optical transmission

maps are to be built, the reference is synchronous to an amplitude modulation of the laser amplitude at a frequency $f' << f$, so that efficient temporal integration over all polarization states is achieved.

In order to enable sensitivity to the local dichroic properties, the polarization state of the laser radiation probing the sample is conditioned by a photo-elastic modulator with small residual static birefringence (PEM, Hinds Instruments PEM100) prior to entering the optical fiber probe. Being the linear laser polarization oriented at 45 degrees with respect to the PEM optical axis, the intensity of the electric field at the PEM output can be written [S3] as

$$\vec{E}_{PEM} = \frac{E_0}{\sqrt{2}}(\hat{e}_x + \exp(i\varphi(t))\hat{e}_y), \quad (1)$$

where $\varphi(t) = A\cos(\omega_m t)$ is the time-dependent optical retardation introduced by the PEM (A is the user-selectable maximum retardation and $\omega_m = 2\pi f$, with f = 50 kHz), $\hat{e}_x$ and $\hat{e}_y$ are the versors of two mutually orthogonal in-plane directions, E_0 is the field amplitude at the PEM input (negligible absorption is assumed).

Figure SI1 illustrates the polarization status of the radiation at the PEM output at selected times. It is clear that the polarization is periodically modified through circular to linear and elliptical. In particular, both right and left circular polarizations are achieved during a single period T=1/f.

Using the basis $\hat{\psi}_{\pm} = \frac{1}{\sqrt{2}}(\hat{e}_x \pm i\hat{e}_y)$ for the circular polarization (either right or left-polarized depending on the ± sign), Eq. 1 can be rewritten as follows:

$$\vec{E}_{PEM} = \frac{E_0}{2}\left((1 - exp(i\varphi(t)))\hat{\psi}_+ + (1 + \mathrm{i}\exp(i\varphi(t)))\hat{\psi}_-\right) \quad (2)$$

Interaction of the so-modulated radiation with a circular dichroic material, showing absorption coefficients α_+ and α_- for right and left circular polarizations, respectively, and thickness z, leads to

$$\vec{E}_{S,C} = \frac{E_0}{2}\left[(1 - i\exp(i\phi(t)))\exp\left(-\alpha_+ \frac{z}{2}\right)\psi_+ + (1 + i\exp(i\phi(t)))\exp\left(-\alpha_- \frac{z}{2}\right)\psi_-\right] \quad (3)$$

that represents the complex amplitude of the electric field after crossing the sample.

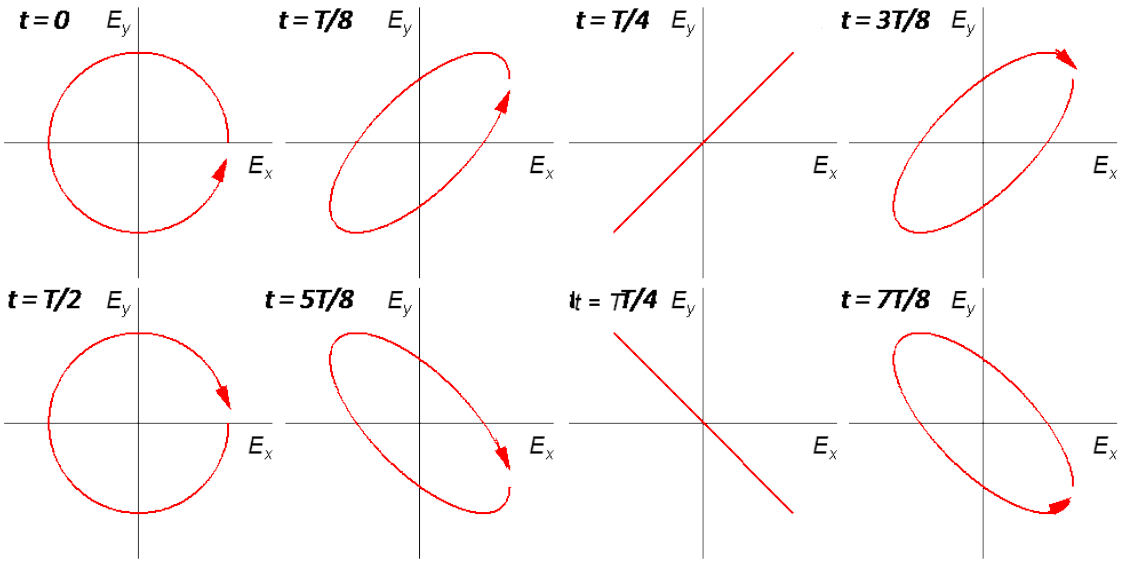

Figure SI1: Polarization at the PEM output. Representation of the polarization of light at the PEM output at some different times, specified in units of the period $T=1/f$ in the plots. E_x and E_y are the amplitude of the electric field along two in-plane mutually orthogonal directions in the lab frame. The arrows indicate the direction of rotation for the electric field vector. Remarkably, both right and left circular polarizations are achieved in a single modulation period.

Assuming a detector with negligible sensitivity on polarization, which has been tested to be the case in our experiment, the transmitted intensity can be written as:

$$I_{S,C} = \left|E_{S,C}\right|^2 = \frac{I_0}{2}\left(\exp(-\alpha_+ z) + \exp(-\alpha_- z)\right) + \sin(\phi(t))\left(\exp(-\alpha_+ z) - \exp(-\alpha_- z)\right) \quad (4)$$

where $I_0 = \left|E_0\right|^2$. The expression above shows that the intensity is given by the sum of a constant term, depending on the polarization-averaged absorption, and a time-dependent term containing

sin(φ(*t*)). In order to identify the relevant harmonic components, expansion of sin(φ(*t*)) in Fourier series can be carried out.[S4] The first term of the expansion, at angular frequency ω_m, reads:

$$I_{I,C} = I_0 J_1(A)(\exp(-\alpha_+ z) - \exp(-\alpha_- z)) \quad (5)$$

where J_1 is the Bessel function of the first order. We note that, unless for choices of the PEM maximum retardation A leading to $J_1(A) = 0$, which is not the case in typical measurements, $I_{I,C}$ is proportional to the difference $\exp(-\alpha_+ z) - \exp(-\alpha_- z)$ between the absorption of right and left circular polarization (circular dichroism). Moreover, the following terms of the Fourier expansion contains odd powers of ω_m, therefore no signal is read when demodulating at the second harmonics.

Let us now consider a sample showing (also) linear dichroism. In particular, we consider a material having absorption coefficients $\alpha_{//}$ and $\alpha_\perp$ for radiation polarized along two mutually orthogonal directions. We assume that one of such directions (whether // or ⊥ is not relevant for our purposes) is oriented at a generic angle ϑ with respect to $\hat{x}$. The corresponding versors are thus $\hat{e}_{//} = (\cos\vartheta\hat{x} + \sin\vartheta\hat{y})/\sqrt{2}$ and $e_\perp = (\sin\vartheta\hat{x} - \cos\vartheta\hat{y})/\sqrt{2}$. By projecting the electric field Eq.1 along the new directions $\hat{e}_{//}$ and $\hat{e}_\perp$, interaction with the sample leads to the following electric field:

$$\mathrm{r}\,\mathrm{E}_{\mathrm{S,L}} = \frac{\mathrm{E}_0}{2}\left((\cos\vartheta + \exp(i\phi(t))\sin\vartheta)\exp\left(-\alpha_{//}\frac{\mathrm{z}}{2}\right)\hat{e}_{//} + (\sin\vartheta - \exp(\mathrm{i}\phi(\mathrm{t}))\cos\vartheta)\exp\left(-\alpha_\perp\frac{z}{2}\right)\hat{e}_\perp\right) \quad (6)$$

corresponding to the intensity

$$\mathrm{I}_{\mathrm{S,L}} = \frac{\mathrm{I}_0}{2}(\exp(-\alpha_{//} z) + \exp(-\alpha_\perp z)) + ((\exp(-\alpha_{//} z) - \exp(-\alpha_\perp z))\sin(2\vartheta)\cos(\phi(t))) \quad (7)$$

Also in this expression we can easily identify a constant term, accounting for the polarization-averaged absorption, and a time dependent contribution, proportional to the difference in

absorption of parallel and orthogonal polarization directions (linear dichroism) and to the angle 2ϑ identifying the geometry of the optical axis of the dichroic material. Such a term is a function of time through cos(φ(*t*)). The latter term can be expanded in Fourier series leading to a constant term ($2J_0(A)$) and a term oscillating at $2\omega_m$ ($2J_2(A)\cos(2\omega_m t)$). We note that by choosing A=2.405=0.383λ, with λ the laser wavelength, as accomplished in our experiment, the constant term of the expansion vanishes. Demodulation at the second harmonics leads to

$$I_{II,L} = I_0 J_2(A)\left(\exp(-\alpha_{//} z) - \exp(-\alpha_{\perp} z)\sin(2\vartheta)\right) \tag{8}$$

Therefore, by splitting the photodetector signal and using two independent lock-in amplifiers demodulating at the first and second harmonics, circular and linear dichroism can be simultaneously measured [S5,S6]. There are, however, a few issues to be duly considered when the method is implemented in a SNOM.

The first one deals with the angle ϑ, which modulates the sensitivity to linear dichroism. We remind that such an angle is inscribed between $\hat{x}$ and $\hat{e}_{//}$ (or $\hat{e}_{\perp}$). We note that the reference direction $\hat{x}$ has to be taken in the in-plane reference frame of the sample, which is different with respect to the laboratory frame. Moreover, when investigating the optical activity of individual entities (the nanoribbons) deposited onto a substrate with no pre-alignment procedure, the direction of the optical axes cannot be defined, or estimated, in advance. This makes a big difference with respect to conventional polarimetry, where the optical axes can usually be pre-defined based on the geometry (anisotropy) of the sample. As a consequence, the quantitative evaluation of the linear dichroism is hampered, unless an independent evaluation of the reference direction is available. This can be estimated by launching linear polarization into the fiber probe and analyzing the near-field radiation with a polarizer placed in front of the photodetector (a non-optical active sample, e.g., a bare substrate, is used in this case). Based on the literature (see, e.g., Ref. [S1]), we know that the direction of the linear polarization at the entrance of the fiber probe is reflected into a specific polarization state in the near-field.

The second issue worth to be discussed addresses the use of near-field probes based on optical fibers. As a matter of fact, the above mentioned relationship between the polarization at the fiber entrance and in the near-field is valid only for selected probes. This is mostly due to the naturally

occurring birefringence of the fiber probe, which can achieve different values for fibers belonging even to the same fabrication batch. In addition, care must be devoted in the experiment to avoid unwanted mechanical stresses to the optical fiber, which might result in fluctuations of birefringence. Scans of bare substrates demonstrated fluctuations within ±5% of the signal in our experimental conditions.

The fiber probe birefringence, as well as the unavoidable spurious optical activity of the components (e.g., mirrors, lenses, beam-splitters) in the optical bench can heavily affect the results. From the point of view of the mathematical description, a constant retardation term φ_{sp} accounting for all spurious birefringence must be added to $\varphi(t)$ appearing in the above equations. By using well known trigonometric formulae, the $\sin(\varphi(t))$ and $\cos(\varphi(t))$ terms appearing in $I_{I,C}$ and $I_{II,L}$, respectively, must be replaced with:

$$\sin(\varphi(t)) \rightarrow \sin(\varphi(t)+\varphi_{SP}) = \sin(\varphi(t))\cos(\varphi_{SP}) + \cos(\varphi(t))\sin(\varphi_{SP}) \quad (9)$$

$$\cos(\varphi(t)) \rightarrow c\cos(\varphi(t)+\varphi_{SP}) = \cos(\varphi(t))\cos(\varphi_{SP}) - \sin(\varphi(t))\sin(\varphi_{SP}) \quad (10)$$

As previously discussed, the ability to independently analyze circular and linear dichroism relies on the Fourier expansion of sine and cosine functions, leading to first and second harmonics components, respectively proportional to differential absorption of circular and linear polarizations. Because of the spurious contribution φ_{SP}, expansion in Fourier series (truncated to the second order, higher harmonics are not significant in the experiment) are modified as follows:

$$\sin(\varphi(t)) \cong J_0(A)\cos(\varphi_{SP}) - 2J_1(A)\sin(\varphi_{SP})\cos(\omega_m t) - 2J_2(A)\cos(\varphi_{SP})\cos(2\omega_m t) \quad (11)$$

$$\cos(\varphi(t)) \cong J_0(A)\sin(\varphi_{SP}) + 2J_1(A)\cos(\varphi_{SP})\cos(\omega_m t) - 2J_2(A)\sin(\varphi_{SP})\cos(2\omega_m t) \quad (12)$$

Therefore, independent measurement of the circular and linear dichroism is possible only if terms containing $\sin(\varphi_{SP})$ are negligible with respect to the other terms in the equations above. In fact, the intensity demodulated at the first and second harmonics (as usual, we neglect both constant and higher harmonics components, not relevant in the experiment), read

$$I_I = I_0 J_I(A)\left(\Delta_C cos(\varphi_{SP}) - \Delta_L sin(\varphi_{sp})\right) \quad (13)$$

$$I_{II} = -I_0 J_2(A)\left(\Delta_C sin(\varphi_{sp}) + \Delta_L cos(\varphi_{sp})\right) \quad (14)$$

where $\Delta_C = \left(\exp(-\alpha_+ z) - \exp(-\alpha_- z)\right)$ and $\Delta_L = \left(\exp(-\alpha_{//} z) - \exp(-\alpha_\perp z)\right)\sin(2\vartheta)$.

Evaluation of the spurious contribution φ_{SP} can be accomplished by repeating the same measurement, i.e., by scanning the same region of the sample, in purposely different experimental conditions. This can be achieved for instance by placing a quarter-wave plate after the PEM, oriented at 90 degrees with respect to the laser polarization direction (hence at -45 degrees with respect to the PEM axis). This produces a further, known and constant, optical retardation term, $\varphi_{\lambda/4} = \pi/2$, which has to be added to φ(*t*) and φ_{SP}. The so introduced π/2 dephasing leads to

$$I_I^{'} = I_0 J_1(A)\left(\Delta_C \sin(\varphi_{SP}) + \Delta_L \cos(\varphi_{SP})\right) \quad (15)$$

$$I_{II}^{'} = I_0 J_2(A)\left(\Delta_C \cos(\varphi_{SP}) - \Delta_L \sin(\varphi_{SP})\right) \quad (16)$$

The value φ_{SP} can hence be retrieved by solving the set of four equations Eqs. (13-16) with the experimental values of the relevant intensities. We have found large variations in the values of φ_{SP} in batches of nominally identical fiber probes, and selected for the measurements probes showing $\varphi_{SP} < 0.2$ rad, that leads to corrections within the estimated uncertainty of the whole procedure in the determination of Δ_C and Δ_L, prudentially set to ±20%. Such estimation accounts for experimental fluctuations, including those related to coupling of the near-field with the material, as well as for the non-direct evaluation of φ_{SP}.

Finally, we note that the optical setup, in particular for the presence of mirrors and beam-splitters whose reflectivity slightly depends on the polarization, produces additional unwanted effects which can be described with a spurious dichroism (this factor takes into account also possible dependence of the photodetector sensitivity on the polarization). Such spurious dichroism leads to a pedestal in the measurement, i.e., a non-zero background signal which is detected also outside the nanoribbons, e.g., on the bare substrate. The effect can be easily removed by adding constant terms to the map, chosen in order to have zero Δ_C and Δ_L values on the bare substrate.

The spurious dichroism has been accounted for in the calibration of the optical near-field maps presented in the paper as well as in the evaluation of the measurement uncertainty.

References

[S1] L. Ramoino, M. Labardi, N. Maghelli, L. Pardi, M. Allegrini, and S. Patanè, Rev. Sci. Instrum. **73**, 2051 (2002).

[S2] K. Karrai and I. Tiemann, Phys. Rev. B **62,** 13174 (2000).

[S3] A.F. Drake, J. Phys. E: Sci. Instrum. **19**, 170 (1986).

[S4] H. Abramowitz and I. Stegun, Handbook of Mathematical Functions (Dover Publications, New York, 1972).

[S5] K.W. Hipps and G.A. Crosby, J. Phys. Chem. **83**, 555 (1979).

[S6] R. Kuroda, T. Harada, and Y. Shindo, Rev. Sci. Instrum. **72**, 3802 (2001).